J Nanopart Res (2009) 11:1321–1330
DOI 10.1007/s11051-008-9534-5

RESEARCH PAPER

A novel magnetic fluid based on starch-coated magnetite nanoparticles functionalized with homing peptide

Ji-Sen Jiang · Zhi-Feng Gan · Yong Yang · Bing Du · Min Qian · Ping Zhang

Received: 19 March 2008 / Accepted: 24 September 2008 / Published online: 24 October 2008

Abstract Preparation and characterization in vitro and in vivo of a novel magnetic fluid based on starch-coated magnetite nanoparticles functionalized with homing peptide is reported in this paper. Precursory magnetic fluids stabilized with starch were prepared, in a polymeric starch matrix, by controlled chemical coprecipitation of magnetite phase from aqueous solutions. The average hydrodynamic diameter of starch-coated iron oxide nanoparticles (SIONs) was 46 nm. As a homing peptide, A54 is the most effective peptide specific to the human hepatocellular carcinoma cell line BEL-7402. Final magnetic fluids were obtained through chemical coupling of homing peptide labeled with 5-carboxyl-fluorescein (FAM-A54) and SIONs. Magnetic measurements showed the saturation magnetization value of SIONs amounted to 45 emu/g and the FAM-A54-coupled SIONs showed a good magnetic response in magnetic field. The results of experiments in vitro and in vivo showed that SIONs were endowed with specific affinity to corresponding tumor cells after coupling with FAM-A54 and the FAM-A54-coupled SIONs could be accumulated in the tumor tissue with more efficiency than individual magnetic targeting or biomolecular targeting. This novel magnetic fluid with dual function has great potential applications in diagnostics and therapeutics of human tumor such as drug targeting, magnetic hyperthermia, and magnetic resonance imaging.

Keywords Magnetic fluid · Dual function · Homing peptide · Nanoparticles coupling · Nanomedicine

J.-S. Jiang (✉) · Z.-F. Gan · Y. Yang
Department of Physics, Center of Functional Nanomaterials and Devices, East China Normal University, North Zhongshan Rd. 3663, Shanghai 200062, People's Republic of China
e-mail: jsjiang@phy.ecnu.edu.cn

B. Du · M. Qian · P. Zhang
School of Life Science, East China Normal University, Shanghai 200062, People's Republic of China

Introduction

Based on the unique magnetic property and biocompatibility, magnetic nanoparticles offer a high potential for several biomedical applications (Gupta and Gupta 2005; Gan and Jiang 2005), such as magnetic cell separation, magnetic resonance imaging (MRI), magnetic hyperthermia, drug targeting, enzyme immobilization, DNA and RNA purification. Advancement in the use of magnetic particles for all these end applications depends on the size and size distribution of particles, surface properties, magnetic properties, and stabilization (Lübbe et al. 1996; Alexiou et al. 2000; Asmatulua et al. 2005). So the synthetic methods and surface engineering of magnetic nanoparticles have become a main research issue in biomedical applications. Most works (Zhang et al. 2002; Xu et al. 2005; Khor and Lim 2003) focused on

coating of magnetic cores with a layer of hydrophilic polymer such as polyethylene glycol (PEG), dextran, chitosan, etc. These biocompatible polymeric coatings on magnetic nanoparticles offer several advantages: (i) The coatings improve the biocompatibility and the stability of the colloid as well as the reticuloendothelial system (RES) evading efficiency; (ii) Polymeric coatings of magnetic particles can bind to various functional biological molecules such as polypeptide, antibodies, enzymes, DNA, and RNA, which encourage the construction of multifunctional nanoparticles.

Homing peptides (Pasqualini and Ruoslahti 1996; Aina et al. 2002), as excellent targeting agents for human tumor, are important in the development of tumor therapeutics. Recently, inorganic nanoparticles modified with homing peptides and their applications in tumor diagnostics and therapeutics have received scientists' attention. Akerman and co-workers have used homing peptides to target i.v.-injected ZnS-capped CdSe quantum dots to specific vascular sites in mice. Their results suggested the potential selective targeting of other nanomaterials in disease diagnosis and therapy (Akerman et al. 2002).

A hepatocarcinoma-binding peptide, AGKGTPSLETTP peptide (A54), which was identified from a phage-display random peptide library by in vivo panning (Qian et al. 2004), is the most effective peptide specific to the human hepatocellular carcinoma cell line BEL-7402. Recently, we have successfully immobilized this homing peptide labeled with green fluorescent protein(A54-GFP)on bare magnetite nanoparticles through the method of hydrogen bonding as well as carbodiimide-mediated esterification between carboxyl group of A54-GFP molecule and hydroxy group on the surface of magnetic nanoparticles (Gan et al. 2008). The A54-GFP-conjugated magnetite nanoparticles possess multifunctional magnetic, tumor cell-specific, and fluorescent properties. However, it is a challenge to prepare a stable magnetic fluid with both high magnetic responsibility and tumor cell-specificity used in vivo. In this study, a novel magnetic fluid based on biocompatible starch-coated iron oxide nanoparticles (SIONs) and homing peptide FAM-A54 was prepared by chemical coupling. The magnetic responsibility and specificity to the human hepatocellular carcinoma cell of the biocompatible FAM-A54-coupled SIONs in the magnetic fluid was studied in vitro and in vivo. The magnetic fluid showed dual function of high magnetic responsibility and cell-specificity and has great potential applications in diagnostics and therapeutics of human tumor in such areas as drug targeting, magnetic hyperthermia, and magnetic resonance imaging.

Materials and methods

Materials

Iron (III chloride hexahydrate ($FeCl_3 \cdot 6H_2O$, >99%), Iron (II sulfate heptahydrate ($FeSO_4 \cdot 7H_2O$, >99%), Sodium hydroxide (NaOH, ≥96%), Sodium metaperiodate ($NaIO_4$, ≥99.5%), Sodium borohydride ($NaBH_4$, >96%) were obtained from Sinopharm Chemical Reagent Co., Ltd (China). All the other chemicals were of analytical grade from local suppliers and used without further purification. Two peptides were used: AGKGTPSLETTP peptide (denoted as A54) and HSYHSHSLLRMF peptide (denoted as C10). A54 is the most effective peptide specific to the human hepatocellular carcinoma cell line BEL-7402. As a contrast, C10 peptide is non-specific to the human hepatocellular carcinoma cell. Both peptides were synthesized by HD Biosciences Ltd (Shanghai, China) and labeled with 5-carboxyl group fluorescein (FAM). Fetal calf serum (FCS) and RPMI 1640 medium were purchased from Invitrogen (Carlsbad, CA, USA). The human hepatocellular carcinoma cell line BEL-7402 and normal liver cell line HL-7702 were purchased from the cell bank of Shanghai Institute for Biological Sciences (Shanghai, China).

Synthesis of starch-coated iron oxide nanoparticles (SIONs)

SIONs were prepared in a polymeric starch matrix, by controlled chemical coprecipitation of magnetite phase from aqueous solutions containing suitable salts of Fe^{2+} and Fe^{3+} mainly based on the Van der Waals reaction between starch and magnetite nanoparticles. Starch (6 g) was dissolved in 40 mL of deionized water at 80 °C. Deionized water was deoxygenated by bubbling with N_2 gas for 1 h prior to use. After the starch was thoroughly dissolved, starch solution was poured into a 24 mL portion of solution containing 0.8 M Fe^{3+} ions and 0.4 M Fe^{2+} ions under vigorous stirring. Then 1.0 M NaOH solution was added dropwise into the mixture

solution of starch and iron salts until the pH of the solution achieved 9–11. N_2 gas was bubbled through the reaction medium during synthesis in a closed system. After 2 h reaction, the resulting black suspension was neutralized with 0.1 M HCl. To remove aggregates, the suspension was centrifugated for 15 min at 1,500 rpm. The prepared SIONs were dialyzed for removal of excess unreacted starch at room temperature for 2–3 days. Finally, the SIONs were washed with deionized water several times and redispersed in phosphate buffer solution and precursory magnetic fluid was obtained. In the magnetic fluid, little free starch exists. Gravimetric analysis showed that starch in the coating layer of SIONs amounted to 20% (wt%).

Coupling of FAM-A54 peptide and SIONs

The aldehyde groups of the starch-coated iron oxide nanoparticles were covalently linked to the amine groups of FAM-A54 by means of Schiff's bases reaction (Bulte et al. 1999) between amine groups of FAM-A54 molecules and the surface aldehyde groups of polyaldehyde-SIONs. In a typical procedure, 2 mL solution of oxidizing agent sodium metaperiodate ($NaIO_4$) was first added to 8 mL SIONs suspension under a N_2 atmosphere. The final concentration of $NaIO_4$ was 5 mM. After reaction in the dark at 4 °C for 5 h, the formed polyaldehyde-SIONs were purified by dialysis against 5 L of deionized water, removing any unbound or released free starch. Then the prepared polyaldehyde-SIONs suspension was diluted to 1 mg/mL with PBS buffer. Afterward, 20 μL FAM-A54 solution with a concentration of 5 mg/mL was added to 1 mL polyaldehyde-SIONs solution to form Schiff's bases at 4 °C for 24 h. The unstable Schiff's bases were reduced to secondary amide bonds by adding 40 μL 0.5 M $NaBH_4$ and incubation at room temperature for 3 h, and the resulting FAM-A54-coupled SIONs solution was dialyzed and redispersed in PBS buffer. This final magnetic fluid will be used in studies in vitro and in vivo.

Specific binding of FAM-A54-coupled SIONs to tumor cells in vitro

To explore the binding activity and specificity of peptide-coupled SIONs in vitro, experiments were conducted. Binding of FAM-A54-coupled SIONs to both the human hepatocellular carcinoma cell line BEL-7402 and normal liver cell line HL-7702 was studied. First, BEL-7402 cell and HL-7702 cell were cultured in RPMI 1640/10% FCS at 37 °C in a humidified atmosphere containing 5% CO_2, and plated into a 24-well plate containing coverslips (1×10^4 cells/well) the day before use. Then FAM-A54-coupled SIONs solution with a particle concentration of 50 μg/mL was added to the cell culture media. After culturing for 2 h, the cells were washed with PBS and examined using fluorescence microscopy. As control experiments, the binding activity and specificity of free FAM-A54 and FAM-C10 were also conducted.

Targeting of FAM-A54-coupled SIONs to tumor tissue in vivo

The experimental animals were nude mice bearing human hepatocellular carcinoma cell BEL-7402 xenografts. Human hepatocellular carcinoma cell BEL-7402 was grafted under the oxter skin of nude mice. Tumor size was about 1 cm when the nude mice were 4–6 weeks old, 20–25 g body weight (purchased from Shanghai Animal Center). The nude mice were anaesthetized slightly and tied on a board. Different magnetic fluid was intravenously injected on the tail of nude mice with the dose of 5 mg/kg body weight. A columned permanent magnet of 0.5 Tesla was fixed on the surface of tumor for 2 h. Then the nude mice were sacrificed by cervical dislocation. Tumor tissue of nude mice was collected, embedded by paraffin and made sections with HE dye. The sections were examined using an Olympus BX51TF fluorescence microscopy. In the entire experiment, 16 nude mice were divided into 4 groups: (1) S1, SIONs solution (precursory magnetic fluid) was intravenously injected without magnetic field applied on the tumor; (2) S2, SIONs solution was intravenously injected with a magnetic field applied on the tumor; (3) S3, FAM-A54-coupled SIONs solution (final magnetic fluid) was intravenously injected without magnetic field applied on the tumor; (4) S4, FAM-A54-coupled SIONs solution was intravenously injected with a magnetic field applied on the tumor.

Approval of animal experiments was obtained from the Science and Technology Commission of Shanghai Municipality (SYXK 2004-0001).

Instrumentation and measurements

The phase composition of samples was characterized by X-ray diffraction (XRD) using D/Max 2250 V diffractometer employing Cu Kα ($\lambda = 0.15418$ nm) radiation. The size and morphology of the particles were measured by a JEM-100CXII transmission electron microscope and JSM 6700F scanning electron microscope (JEOL, Japan). The microstructure of the samples was investigated by Mössbauer spectroscopy using a constant-acceleration spectrometer with a ^{57}Co source in a Pd matrix at room temperature. The spectrometer (Wissel, Germany) was calibrated using a standard 25 μm α-Fe foil. The UV-vis absorption spectra of samples was measured using a Unico UV-2802S UV-Vis spectrometer. The magnetic properties of samples at room temperature were measured by HH-15 vibrating sample magnetometer. Fluorescence microscopy was performed with an Olympus BX51TF microscope with a cooled frame CCD camera for FAM with excitation and emission wavelengths of 490 and 520 nm, respectively, and Image-pro Plus 5.0 image analysis software.

Results and discussion

Structure and morphology of SIONs

The SIONs are composed of iron oxide core and starch chains coating the core. Both XRD and Mössbauer Spectroscopy were used to obtain structure information of SIONs before and after oxidating. Figure 1a shows the XRD patterns of SIONs. The position and relative intensity of XRD peaks of sample is in good agreement with standard XRD card (JCPDS: 19-629) of magnetite, indicating the core of SIONs consisted of cubic phase Fe_3O_4. Using Scherrer's formula, the crystallite size of magnetite core was estimated to be about 7 nm. Besides, some new diffraction peaks at lower degree of $2\theta = 15$–$20°$ may be attributed to the crystal peak of surface starch layer (Matveev et al. 2001). Compared to the sample of SIONs, no new diffraction peaks are observed in the sample of polyaldehyde-SIONs (Fig. 1b). This result indicates that although SIONs were perioxidated by periodate, $NaIO_4$ has no evident effect on the crystal structure of magnetite core. Figure 2 shows the room temperature Mössbauer spectra of

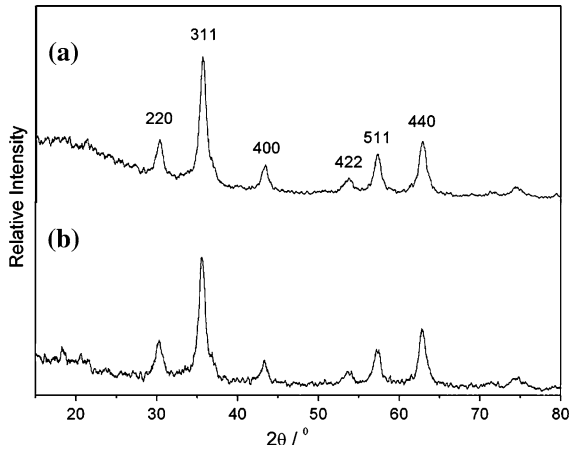

Fig. 1 The X-ray diffraction patterns of samples: **a** starch-coated iron oxide nanoparticles (SIONs) and **b** polyaldehyde-SIONs

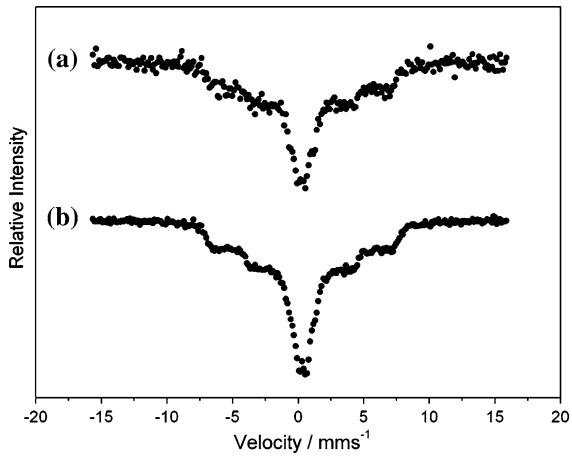

Fig. 2 The Mössbauer Spectra of samples at room temperature: **a** starch-coated iron oxide nanoparticles (SIONs) and **b** polyaldehyde-SIONs

samples before and after oxidating. Both the two spectra reflect superparamagnetic relaxation behavior in the case of 7 nm Fe_3O_4 nanocrystallites coated with the biopolymer. Compared to SIONs, the doublet spectrum area of polyaldehyde-SIONs has increased apparently, which indicates the periodate oxidation has effect on the relaxation behavior of the sample. When starch-coating layers of SIONs were perioxidated by periodate, some of the alcohol groups of starch chains converted to aldehyde groups, which change the chemical environment of atoms at the surface of magnetite cores (Yang et al. 1992).

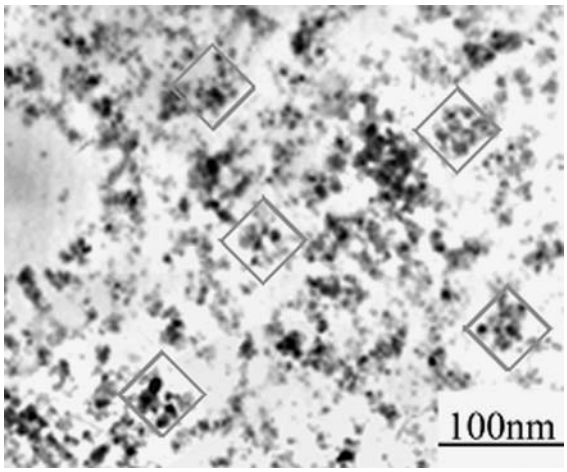

Fig. 3 TEM image of starch-coated iron oxide nanoparticles (SIONs)

The morphology of SIONs is shown in Fig. 3 through a TEM micrograph. Electron-dense magnetite cores were clearly seen as dark regions in the micrograph. Their average diameter was 8 nm. Figure 4 shows an SEM image of SIONs. Most of the particles are quasi-spherical. The mean size of particles fluctuates from 40 to 50 nm.

From the results of particle size analysis of the SEM and TEM images of SIONs, we conclude that an individual starch-coated iron oxide nanoparticle is composed of several magnetite cores and starch chains coating these cores, which are showed in the panes of Fig. 3. Besides, the inset of Fig. 4 shows the particle size distribution of the samples. The average

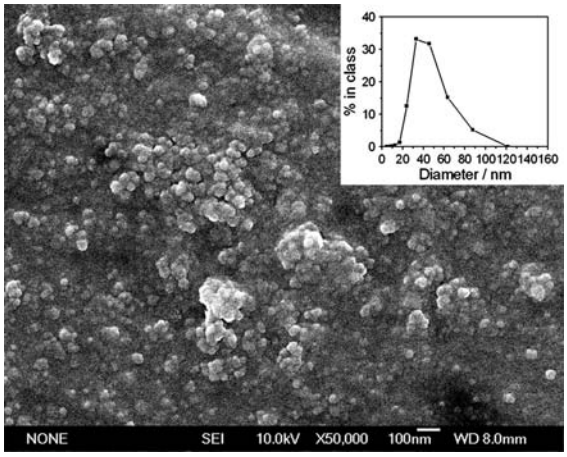

Fig. 4 SEM image of starch-coated iron oxide nanoparticles (SIONs) and particles size distribution of SIONs (inset)

hydrodynamic diameter of SIONs upon photon correlation spectroscopy (PCS) analysis is 46 nm, which is in agreement with the SEM result.

Coupling of FAM-A54 peptide and SIONs

Natural starch is a branched, hydrophilic, and cross-linked polymer that consists of two major molecular components, amylose (20–30%) and amylopectin (70–80%), both of which are polymers of α-D-glucose units in the $^4C_1$ conformation. In amylose, these are linked -(1 → 4)-, with the ring oxygen atoms all on the same side, whereas in amylopectin about one residue in every twenty is linked -(1 → 6)- forming branch-points. Starch molecules are inert to most direct reactions with biopolymer, and they must be chemically activated to introduce active functional groups. Of note, the hydroxyl groups extensively present in starch are free and can be converted to aldehyde groups via oxidating. The method of our experiment, which introduces active functional groups at random positions in starch, is to cleave the sugar rings with periodates to form polyaldehyde–starch coating layer. So the FAM-A54 has the flexibility to couple with polyaldehyde-SIONs by means of Schiff's bases reaction (Bulte et al. 1999) between amine groups of FAM-A54 molecules and the surface aldehyde groups of polyaldehyde-SIONs.

A 2,4-dinitrophenylhydrazine method (Hong et al. 2004) was utilized to directly detect the periodate-oxidated magnetic polyaldehyde-SIONs. When several drops of polyaldehyde-SIONs solution were added to 2 mL of freshly prepared 2,4-dinitrophenylhydrazine solution, a clear yellow-orange precipitate was obtained. A contrast experiment was also carried out in the same conditions for SIONs solution without oxidating. No precipitate was observed. These results indicate the free hydroxyl groups of starch chains in the coating layer of SIONs converted to aldehyde groups. FAM-A54-coupled SIONs were visualized using fluorescence microscopy (Fig. 5). FAM-A54-coupled SIONs were collected by sedimentation with the help of an external magnetic field. After washing away the physically absorbed FAM-A54 on the SIONs by PBS, we used deionized water to sequentially wash the FAM-A54-coupled SIONs. Then the nanoparticles were put on the slide. Due to the limited magnifying power of Fluorescence Microscope and the method of sample preparation, the results of image

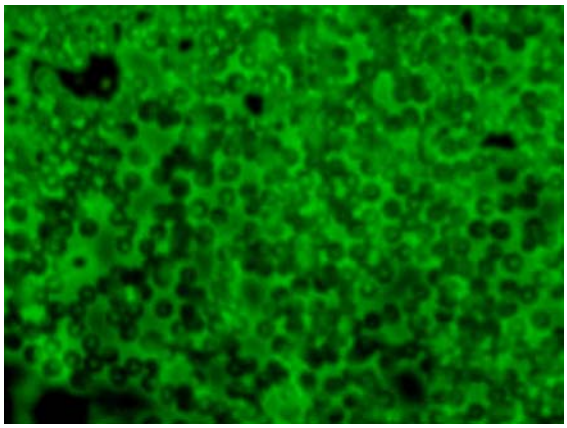

Fig. 5 Fluorescent image of polyaldehyde-SIONs. (×1,000)

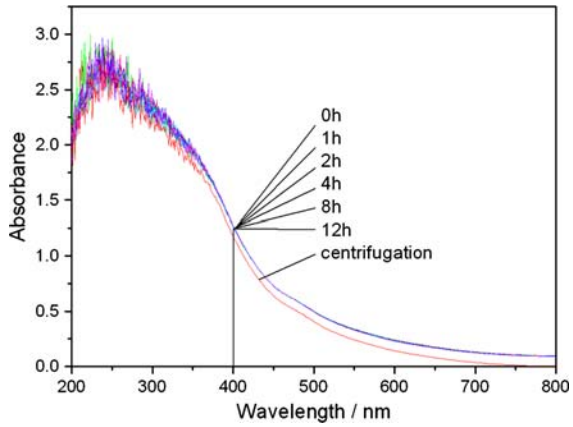

Fig. 6 UV-vis absorption spectra of SIONs suspensions, particles in PBS (0.1 mg/mL)

analysis are small aggregates of FAM-A54-coupled SIONs. Of note, small aggregates have an obvious fluorescence layer on the surface of the samples. This result indicates the immobilization of FAM-A54 on the surfaces of SIONs.

Stability of magnetic fluids

The solution of SIONs dispersed in PBS (pH = 7.4) is a biocompatible magnetic fluid. The stability of magnetic fluid was followed by determinations as a function of time with a UV-vis spectrophotometer. Figure 6 shows the UV-vis absorption spectra of SIONs solution as a function of time. The centrifugal separation was 2,000 rpm for 15 min. Since the absorbance of colloid related to the concentration of nanoparticles in the aqueous media (Plaza et al. 2001), the fact that the absorbance of sample at a certain wavelength of 400 nm was almost constant over 12 h, implied that no obvious sedimentation took place during the observational process. In addition, even after centrifugal separation, the absorbance of sample only decreased slightly. Besides, the magnetic fluids produced in a starch matrix exhibited extremely stable behavior for more than 2 months at room temperature. These facts indicate starch-stabilized magnetic fluids possess excellent stability.

Some works (Xu et al. 2005; Kim et al. 2003) demonstrated the electrostatic repulsion induced by carbohydrate coating of the iron oxide nanoparticles was only slightly stronger than that of uncoated iron oxide nanoparticles at pH around 7–7.5, i.e., the physiological range in the living organisms. So the starch-coated iron oxide nanoparticles seem to be mainly stabilized by steric repulsion (Berry1 and Curtis 2003). The starch-coated iron oxide nanoparticles have a flat layer and longer polymeric chains. When two particles with polymer layer approach one another, the configuration entropy of polymer molecule chains will decrease along with the number of configuration figure due to limited room, which results in steric repulsion. This effect restrained the Van der Waals force and magnetic dipole-dipole attractions between particles, resulting in high stability.

Magnetic properties

The plots of magnetization versus magnetic field (*M–H* loop) at room temperature for the SIONs and polyaldehyde-SIONs are illustrated in Fig. 7a. Saturation magnetization (*M*s), remanent magnetization (*M*r), and coercivity (*H*c) could be determined to be 45 emu/g, 2 emu/g, and 18 Oe, respectively, for SIONs. Both the remanent magnetization and coercivity of the sample are very weak indicating that most of SIONs core is very small and near superparamagnetic. These results are consistent with the result obtained by XRD and Mössbauer Spectroscopy. The saturation magnetization of magnetite nanoparticles was reduced to near 50% of the bulk magnetite (Zaitsev et al. 1999). This is mainly attributed to the existence of non-magnetic materials (starch) on the surface of particles. In addition, this is also caused by the small size effect of nanoparticles, that is, the *Ms* value decreases as the size of particles decreases.

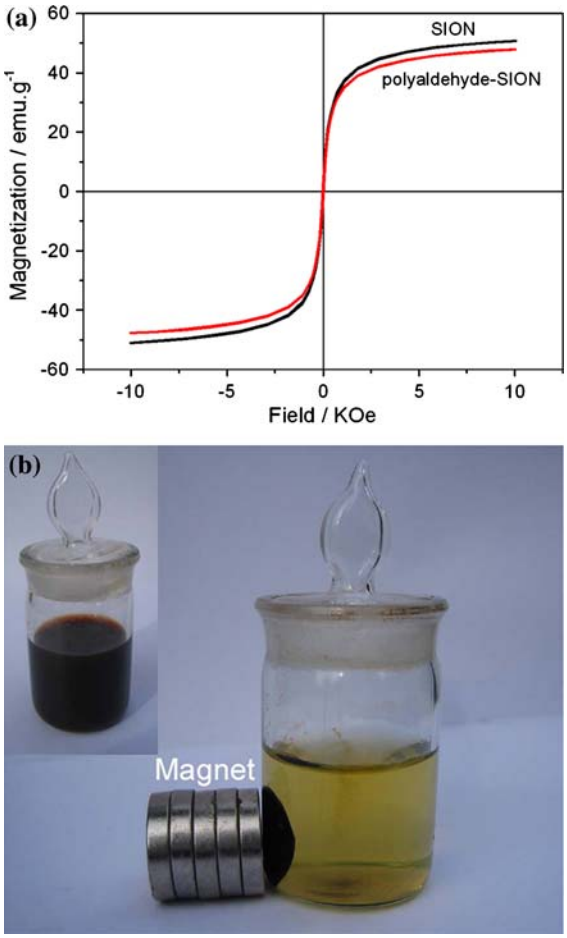

Fig. 7 Magnetic properties of samples: **a** room temperature magnetization curve of starch-coated iron oxide nanoparticles (SIONs) and polyaldehyde-SIONs, **b** magnetic response of FAM-A54-coupled SIONs under an external magnetic field

Besides, surface spin pinning effect (Chen and Liao 2002) also might reduce the *Ms* value of SIONs due to chemisorption of starch molecules on the magnetite cores. Compared to the SIONs, the *Ms* value of polyaldehyde-SIONs only reduce by 2%, which suggests the periodate oxidation has little effect on magnetic property of SIONs. These particles show much the same *Ms* value as folic acid-conjugated magnetite nanoparticles (Mohapatra et al. 2007) and much higher *Ms* value than that of lactobionic acid-modified magnetite nanoparticles (Selim et al. 2007).

The magnetic response of FAM-A54-coupled SIONs in PBS was tested by placing a magnet near the glass bottle. The magnet created a magnetic field with strength of 3.5 KOe. The black particles were attracted toward the magnet within 0.5 h (Fig. 7b), demonstrating directly that the FAM-A54-coupled SIONs possess excellent magnetic response.

Specificity in vitro

Fig. 8a and b show that after intensive washing, FAM-A54 peptide was observed decorating the surface of hepatocellular carcinoma cells, but not FAM-C10 with hepatocellular carcinoma cells. These results demonstrated the specificity of A54 to hepatocellular carcinoma cells. FAM-A54-coupled SIONs were observed decorating the surface of hepatocellular carcinoma cells (Fig. 8c), whereas no visible signal was observed on the normal liver cells (Fig. 8d). These results demonstrated that FAM-A54 still remained specific to hepatocellular carcinoma cells after being chemically coupled with SIONs, so that SIONs coupled with homing peptides were endowed with specific affinity to corresponding tumor cells in vitro.

Targeting in vivo

Figure 9 shows the microscopy images of the tumor tissues of nude mice in different groups. There were no SIONs observed in the tumor tissue after precursory magnetic fluid was intravenously injected in nude mice without a magnetic field applied on the tumor for 2 h (Fig. 9a). It indicates that SIONs are non-specific to human hepatocellular carcinoma cell. Attracted by a magnetic field applied on the tumor for 2 h, SIONs were observed in the tumor interstitial (S2 group, Fig. 9b). This proves SIONs can be delivered to tumor tissue and accumulated in the target area through magnetic targeting. Figure 9c shows accumulation of FAM-A54-coupled SIONs in the tumor tissue after the magnetic fluid was intravenously injected in nude mice without application of a magnetic field. This means that the homing peptide still possess tumor cell-specific after coupled with SIONs in vivo. Figure 9d shows that with a magnetic field applied on the tumor for 2 h, a mass of FAM-A54-coupled SIONs was accumulated in the tumor tissue after FAM-A54-coupled SIONs magnetic fluid was intravenously injected in nude mice. This could be attributed to dual function of both magnetic targeting and biomolecular targeting of FAM-A54-coupled SIONs. The dual functional FAM-A54-coupled SIONs successfully inherit the advantages of magnetic targeting and

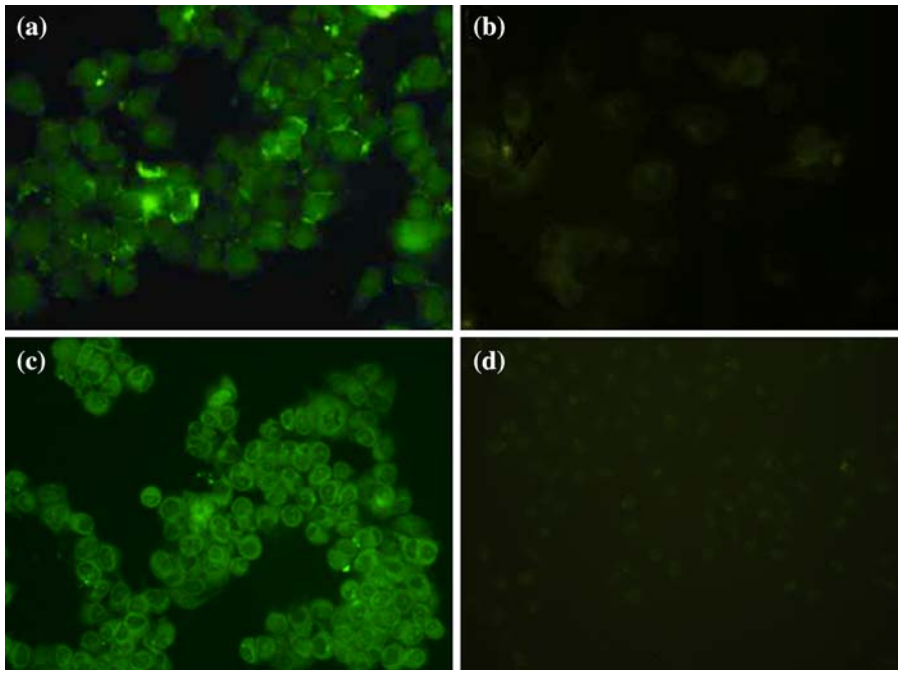

Fig. 8 Fluorescent images of **a** binding of free FAM-A54 to the human hepatocellular carcinoma cell, **b** binding of free FAM-C10 to the human hepatocellular carcinoma cell, **c** binding of FAM-A54-coupled SIONs to the human hepatocellular carcinoma cell, **d** binding of FAM-A54-coupled SIONs to the normal liver cell. (Original magnifications: ×400)

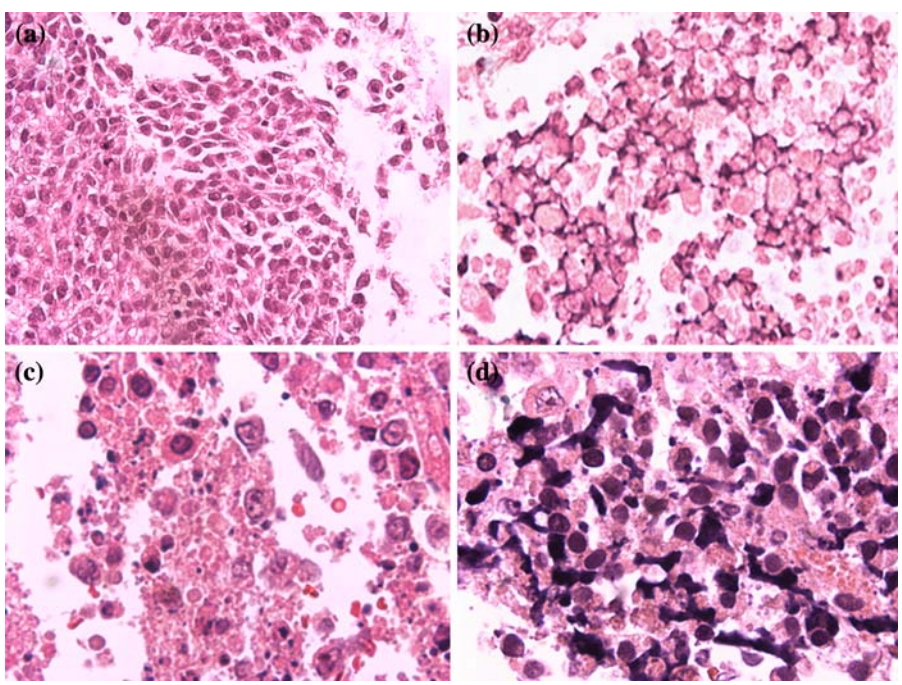

Fig. 9 Photomicrographs of the tumor tissues of nude mice injected with different magnetic fluid with or without external magnetic field: **a** SIONs magnetic fluid without magnetic field; **b** SIONs magnetic fluid with magnetic field; **c** FAM-A54-coupled SIONs magnetic fluid without magnetic field; **d** FAM-A54-coupled SIONs magnetic fluid with magnetic field

biomolecular targeting, so that these nanoparticles can be targeted in the tumor tissue with more efficiency than individual magnetic targeting or biomolecular targeting. In addition, compared with the solution of A54-GFP (homing peptide labeled with green fluorescent protein)-coated magnetite nanoparticles (without starch) (Gan et al. 2008), these magnetic targeting particles showed high stability when used in vivo.

Conclusion

The results described in this study present a novel magnetic fluid based on starch-coated iron oxide (Fe_3O_4) nanoparticles functionalized with homing peptide. The SIONs are composed of iron oxide core and starch chains coating the core. The average magnetite core size of 7 nm was found by XRD and that of 8 nm was found by TEM. Most of starch-coated iron oxide nanoparticles are quasi-spherical with average hydrodynamic diameter of 46 nm. The SIONs dispersing in PBS (pH = 7.40) possess excellent stability. Coupling of homing peptide labeled with 5-carboxyl-fluorescein (FAM-A54) and SIONs was achieved by Schiffs' reaction. Magnetic measurements showed the saturation magnetization value of SIONs amounted to 45 emu/g and the FAM-A54-coupled SIONs showed a good magnetic response in the magnetic field. The results of the experiments conducted in vitro and in vivo showed that the FAM-A54-coupled SIONs magnetic fluid possessed dual function of both magnetic targeting and biomolecular targeting, so that FAM-A54-coupled SIONs can be targeted in the tumor tissue with more efficiency than individual magnetic targeting or biomolecular targeting. This novel magnetic fluid has great potential applications in diagnostics and therapeutics of human tumor in such areas as drug targeting, magnetic hyperthermia, and magnetic resonance imaging.

Acknowledgment This research project is supported by Shanghai Nanotechnology Promotion Center (0352nm113, 0852nm03200).

References

Aina OH, Sroka TC, Chen ML, Lam KS (2002) Therapeutic cancer targeting peptides. Biopolymers 66(3):184–199. doi:10.1002/bip.10257

Akerman ME, Chan WCW, Laakkonen P, Bhatia SN, Ruoslahti E (2002) Nanocrystal targeting in vivo. Proc Natl Acad Sci USA 99(2):12617–12621. doi:10.1073/pnas.152463399

Alexiou C, Arnold W, Klein RJ, Parak FG, Hulin P, Bergemann C, Erhardt W, Wagenpfeil S, Lübbe AS (2000) Locoregional cancer treatment with magnetic drug targeting. Cancer Res 60:6641–6648

Asmatulua R, Zalichb MA, Claus RO, Riffleet JS (2005) Synthesis, characterization and targeting of biodegradable magnetic nanocomposite particles by external magnetic fields. J Magn Magn Mater 292:108–109. doi:10.1016/j.jmmm.2004.10.103

Berryl CC, Curtis ASG (2003) Functionalisation of magnetic nanoparticles for applications in Biomedicine. J Phys D Appl Phys 36:R198–R206

Bulte JWM, Zhang SC, van Gelderen P, Herynek V, Jordan EK, Duncan ID, Frank JA (1999) Neurotransplantation of magnetically labeled oligodendrocyte progenitors: MR tracking migration and myelination. Proc Natl Acad Sci USA 96(26):15256–15261. doi:10.1073/pnas.96.26.15256

Chen DH, Liao MH (2002) Preparation and characterization of YADH-bound magnetic nanoparticles. J Mol Catal B Enzym 16:283–291. doi:10.1016/S1381-1177(01)00074-1

Gan ZF, Jiang JS (2005) Preparation of magnetic monodisperse nanoparticles and biopolymer assemble on the magnetic carriers. Prog Chem 17(6):978–986

Gan ZF, Jiang JS, Yang Y, Du B, Qian M, Zhang P (2008) Immobilization of homing peptide on magnetite nanoparticles and its specificity in vitro. J Biomed Mater Res A 84A(1):10–18. doi:10.1002/jbm.a.31181

Gupta AK, Gupta M (2005) Synthesis and surface engineering of iron oxide nanoparticles for biomedical applications. Biomaterials 26:3995–4021. doi:10.1016/j.biomaterials.2004.10.012

Hong X, Guo W, Yuan H, Li J, Liu Y, Ma L, Bai Y, Li T (2004) Periodate oxidation of nanoscaled magnetic dextran composites. J Magn Magn Mater 269:95–100. doi:10.1016/S0304-8853(03)00566-3

Khor E, Lim LY (2003) Implantable applications of chitin and chitosan. Biomaterials 24(13):2339–2349. doi:10.1016/S0142-9612(03)00026-7

Kim DK, Mikhaylova M, Wang FH, Kehr J, Bjelke B, Zhang Y, Tsakalakos T, Muhammed M (2003) Starch-coated superparamagnetic nanoparticles as MR contrast agents. Chem Mater 15:4343–4351. doi:10.1021/cm031104m

Lübbe AS, Bergemann C, Huhnt W, Fricke T, Riess H, Brock JW, Huhn D (1996) Preclinical experiences with magnetic drug targeting: tolerance and efficacy. Cancer Res 56:4694–4701

Matveev YI, van Soest JJG, Nieman C, Wasserman LA, Protserov VA, Ezernitskaja M, Yuryev VP (2001) The relationship between thermodynamic and structural properties of low and high amylose maize starches. Carbohydr Polym 44:151–160. doi:10.1016/S0144-8617(00)00211-3

Mohapatra S, Mallick SK, Maiti TK, Ghosh SK, Pramanik P (2007) Synthesis of highly stable folic acid conjugated magnetite nanoparticles for targeting cancer cells. Nanotechnology 18:1–9

Pasqualini R, Ruoslahti E (1996) Organ targeting in vivo using phage display peptide libraries. Nature 380(6572):364–366. doi:10.1038/380364a0

Plaza RC, Vicente JD, Gómez-Lopera S, Delgado AV (2001) Stability of dispersions of colloidal nickel ferrite spheres. J Colloid Interface Sci 242:306–313. doi:10.1006/jcis.2001.7882

Qian M, Zhou ZL, Zhang P, Du B, Yu J, Yu M (2004) A hepatocarcinoma-binding peptide from a phage-display random peptide library identified by in vivo panning and its application. Chinese Patent No. 1563077

Selim KMK, Ha YS, Kim SJ, Chang Y, Kim TJ, Lee GH, Kang IK (2007) Surface modification of magnetite nanoparticles using lactobionic acid and their interaction with hepatocytes. Biomaterials 28:710–716. doi:10.1016/j.biomaterials.2006.09.014

Xu XQ, Shen H, Xu JR, Xu J, Li XJ, Xiong XM (2005) Core-shell structure and magnetic properties of magnetite magnetic fluids stabilized with dextran. Appl Surf Sci 252:494–500. doi:10.1016/j.apsusc.2005.01.027

Yang X, Jiang J, Jing J, Hsia YF, Hu Z, Chen X, He Y (1992) Influence of solvent on the superparamagnetic relaxation of nanocrystalline Fe_3O_4 in ferrofluids. Hyperfine Interact 70:1129–1132. doi:10.1007/BF02397528

Zaitsev VS, Filimonov DS, Presnyakov IA, Gambino RJ, Chu B (1999) Physical and chemical properties of magnetite and magnetite-polymer nanoparticles and their colloidal dispersions. J Colloid Interface Sci 212:49–57. doi:10.1006/jcis.1998.5993

Zhang Y, Kohler N, Zhang M (2002) Surface modification of superparamagnetic magnetite nanoparticles and their intracellular uptake. Biomaterials 23(7):1553–1561. doi:10.1016/S0142-9612(01)00267-8